Molecular Biology of the Cell
Vol. 16, 4243–4255, September 2005

Stochastic Simulation of Neurofilament Transport in Axons: The "Stop-and-Go" Hypothesis[V]

Anthony Brown,* Lei Wang,† and Peter Jung‡

*Center for Molecular Neurobiology and Department of Neuroscience, The Ohio State University, Columbus, OH 43210; †Developmental Neurobiology Program, The Burnham Institute, La Jolla, CA 92037; and ‡Department of Physics and Astronomy, Ohio University, Athens, OH 45701

Submitted February 19, 2005; Revised June 22, 2005; Accepted June 23, 2005
Monitoring Editor: Erika Holzbaur

According to the "stop-and-go" hypothesis of slow axonal transport, cytoskeletal and cytosolic proteins are transported along axons at fast rates but the average velocity is slow because the movements are infrequent and bidirectional. To test whether this hypothesis can explain the kinetics of slow axonal transport in vivo, we have developed a stochastic model of neurofilament transport in axons. We propose that neurofilaments move in both anterograde and retrograde directions along cytoskeletal tracks, alternating between short bouts of rapid movement and short "on-track" pauses, and that they can also temporarily disengage from these tracks, resulting in more prolonged "off-track" pauses. We derive the kinetic parameters of the model from a detailed analysis of the moving and pausing behavior of single neurofilaments in axons of cultured neurons. We show that the model can match the shape, velocity, and spreading of the neurofilament transport waves obtained by radioisotopic pulse labeling in vivo. The model predicts that axonal neurofilaments spend ~8% of their time on track and ~97% of their time pausing during their journey along the axon.

INTRODUCTION

Neurofilaments are transported along axons toward the axon tip in the slowest component of axonal transport at average rates of ~0.004–0.04 μm/s, several orders of magnitude slower than the rate of fast axonal transport (Lasek *et al.*, 1992; Nixon, 1998). Numerous studies on neurofilament transport using radioisotopic pulse labeling spanning almost three decades have demonstrated that the pulse of radiolabeled neurofilament proteins moves out along axons in the form of a bell-shaped wave that spreads as it moves distally. These waves have become universally familiar in the field of axonal transport but little is known about how they are generated and what mechanistic significance can be ascribed to their shape.

One early model of slow axonal transport considered that neurofilaments move unidirectionally in a slow and continuous manner (Lasek *et al.*, 1984). In a mathematical description of this model, Blum and Reed (1989) proposed the existence of a hypothetical "engine" that moves at a constant slow velocity of 1 mm/d. Microtubules were considered to interact directly with the engine and neurofilaments were considered to move by piggy-backing on the moving microtubules. According to this model, the average velocity of neurofilament movement was dependent on the equilibrium constants of the interactions between neurofilaments and microtubules and between microtubules and the engine. On the basis of these assumptions, the authors derived a system of partial differential equations to describe slow axonal transport in vivo. By computer simulation of the equations of the model, the authors demonstrated that they could generate transport kinetics similar to those observed in radioisotopic pulse-labeling experiments.

In recent years, considerable progress has been made in the study of neurofilament transport in axons and it is now clear that the motile behavior is quite different from the behavior modeled by Blum and Reed. Specifically, direct observations on neurofilaments in axons of cultured primary neurons using fluorescence microscopy have demonstrated that these polymers actually move at rates of ~0.4–0.6 μm/s, approaching the rate of fast axonal transport and that these rapid movements are also intermittent, bidirectional and highly asynchronous (Wang *et al.*, 2000; Roy *et al.*, 2000; Yabe *et al.*, 2001; Wang and Brown, 2001; Ackerley *et al.*, 2003). Based on these observations, it has been proposed that axonal neurofilaments are actually transported by fast motors and that the overall rate of movement is slow because the filaments spend some of their time moving retrogradely and most of their time not moving at all. In other words, the slow rate of movement is an average of rapid bidirectional movements interrupted by prolonged pauses. We refer to this as the stop-and-go hypothesis of slow axonal transport, and we speculate that it may also explain the slow movement of other cytoskeletal and cytosolic proteins that are conveyed by slow axonal transport (Brown, 2000). This hypothesis combines features of two longstanding competing hypotheses, the unitary hypothesis of Ochs (1975) and the structural hypothesis of Lasek (Tytell *et al.*, 1981), and thus it may go some way to reconciling those two apparently disparate perspectives.

A critical test of the stop-and-go hypothesis is whether it can explain the radioisotopic pulse-labeling kinetics in vivo. Specifically, can the rapid infrequent movements of neurofilaments observed in cultured neurons on a time scale of

This article was published online ahead of print in *MBC in Press* (http://www.molbiolcell.org/cgi/doi/10.1091/mbc.E05–02–0141) on July 6, 2005.

[V] The online version of this article contains supplemental material at *MBC Online* (http://www.molbiolcell.org).

Address correspondence to: Anthony Brown (brown.2302@osu.edu).

seconds or minutes account for the kinetics of movement of populations of neurofilaments observed in living organisms on a time scale of weeks or months? Because it is presently not possible to examine the behavior of individual neurofilaments in vivo, we have used a computational modeling approach. Here we present a stochastic model of neurofilament transport in axons based on a detailed kinetic analysis of the moving and pausing behavior of individual neurofilaments observed in cultured nerve cells. We propose that neurofilaments move along cytoskeletal tracks, exhibiting short bouts of rapid movement interrupted by short "on-track" pauses and that they can temporarily disengage from their tracks, resulting in more prolonged "off-track" pauses. Our model predicts that axonal neurofilaments spend 8% of their time on track and 97% of their time pausing during their journey along the axon. Thus the bidirectional stop-and-go movements of neurofilaments observed by fluorescence microscopy in cultured neurons can explain the kinetics of neurofilament transport observed by radioisotopic pulse labeling in vivo.

METHODS

A Model for Neurofilament Transport

We consider that neurofilaments are cargo structures that move intermittently in both anterograde and retrograde directions along cytoskeletal tracks. The movements in both directions are rapid, but the overall rate is slow because the filaments spend most of their time pausing. Our studies on cultured neurons indicate that each neurofilament appears to have a single preferred direction of movement and that reversals are rare (Wang *et al.*, 2000; Wang and Brown, 2001). For example, most filaments that pause subsequently resume movement in the same direction in which they were moving before pausing. Thus we assume that neurofilaments can switch between two relatively persistent directional states, anterograde or retrograde, and that neurofilaments can move or pause in either state. The net direction is anterograde because neurofilaments spend more time moving anterogradely than retrogradely. As a first approximation, we assume that the transport properties of the neurofilaments do not vary with respect to location along the axon. We also assume that the axon is long so that we can ignore events at the proximal and distal ends.

In our experimental studies, the neurofilaments that we tracked spent ~70% of their time pausing (Wang *et al.*, 2000; Wang and Brown, 2001). However, we have noted previously that these studies underestimated the true overall pausing behavior (Wang *et al.*, 2000). The reason for this is that our measurements relied on the observation of short gaps in the neurofilament array and we were only able to track neurofilaments that moved into these gaps during the period of observation. The fact that the edges of the gaps remained fixed throughout most of our movies indicates that many filaments flanking the gaps paused throughout the observation period, yet we were unable to track these filaments because they could not be resolved from their neighbors. To explain these observations, we propose that in each directional state (anterograde or retrograde), axonal neurofilaments can switch between two additional states: a state in which neurofilaments alternate between bouts of rapid movement interrupted by short pauses, corresponding to the motile behavior observed in our live cell imaging studies, and a state in which neurofilaments pause for more prolonged periods without any movement. For the purposes of this model, we refer to these states as on track and off track.

Assignment of Rate Constants and Probabilities

Assuming that neurofilaments can be either anterograde or retrograde and either on track or off track, we can define four distinct kinetic states: on track in the anterograde state, off track in the anterograde state, on track in the retrograde state and off track in the retrograde state (Figure 1). To determine whether neurofilaments are in the anterograde or retrograde state, we define a reversal rate constant k_{AR}, which represents the average number of times per second that an anterograde filament becomes retrograde, and a reversal rate constant k_{RA}, which represents the average number of times per second that a retrograde filament becomes anterograde. We also define an overall reversal rate, $k_{REV} = k_{AR} + k_{RA}$. To determine whether the neurofilaments are on or off track, we define a rate constant k_{OFF}, which represents the average number of times per second that an on-track filament moves off track, and a rate constant k_{ON}, which represents the average number of times per second that an off-track filament moves on track. As a first approximation, we assume that these rate constants are the same for both anterograde and retrograde filaments. Because the simulations in the present study were all performed using a fixed time interval, we express the rate constants as events per time interval rather than per second.

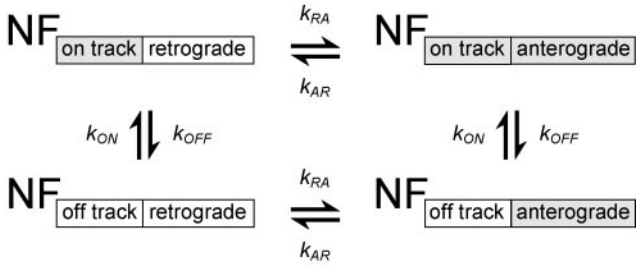

Figure 1. A model for neurofilament transport. We propose that neurofilaments can switch between four states: on track in the anterograde state, off track in the anterograde state, on track in the retrograde state, and off-track in the retrograde state. Neurofilaments that are on track alternate between brief bouts of rapid movement and short pauses, whereas those that are off track are temporarily incapable of movement and exhibit more prolonged pauses. The moving and pausing behavior of the on-track neurofilaments is dictated by the transition probabilities obtained from our original live-cell imaging data (see Table 1). k_{ON} and k_{OFF} are the rates of moving on and off track, respectively (as a first approximation, we assume that these rates are the same for filaments in both the anterograde and retrograde states). k_{AR} is the rate that neurofilaments switch from the anterograde state to the retrograde state and k_{RA} is the rate that neurofilaments switch from the retrograde state to the anterograde state (we assume that these rates are the same for both the on-track and off-track states). Note that neurofilaments can exist in the anterograde and retrograde states when they are on and off track but they can only move when they are on track.

Observations on neurofilaments in cultured nerve cells indicate that the moving and pausing behavior shows no apparent regularity or predictability that might imply a deterministic mechanism. Thus we assume that the moving and pausing behavior can be modeled as a stochastic process described by a series of transition probabilities. Assuming that the transitions of neurofilaments between the on track and off track states are described by a two-state master equation (Van Kampen, 1981), the proportion of filaments that are on track (i.e., the probability of being on track) is given by the ratio $p_{ON} = k_{ON}/(k_{ON} + k_{OFF})$ and the proportion that are off track (i.e., the probability of being off track) is given by the ratio $p_{OFF} = k_{OFF}/(k_{ON} + k_{OFF})$. Similarly, the proportion of filaments in the retrograde state (i.e., the probability of being in the retrograde state) is given by the ratio $p_R = k_{AR}/(k_{AR} + k_{RA})$ and the proportion in the anterograde state (i.e., the probability of being in the anterograde state) is given by the ratio $p_A = k_{RA}/(k_{AR} + k_{RA})$.

Calculation of Transition Probabilities for the Moving and Pausing Behavior

An important feature of neurofilament movement that we have noted in our live cell imaging studies is that there is a persistence to their motile behavior. Rather than switching randomly between moving and pausing states without memory, the filaments tend to alternate between bouts of sustained movement and bouts of sustained pausing. This can be seen by visual inspection of the traces for individual neurofilaments, such as those shown in Figure 4, F–J. Thus the probability of a filament moving in any given time interval is greater if it was moving in the previous time interval than if it was pausing in the previous time interval. Conversely, the probability of a filament pausing in any given time interval is greater if it was pausing in the previous time interval than if it was moving in the previous time interval. Depending on the probabilities of switching between the moving and pausing states, this kind of behavior can be described as a Markovian process, i.e., one in which the behavior in any one time interval is dependent on the behavior in the preceding time interval.

To determine the probability that an on-track neurofilament pauses or moves at a particular speed, we performed a more detailed analysis of the moving and pausing behavior of 72 neurofilaments that we tracked in our previously published study of the movement of neurofilaments in photobleached axons (Wang and Brown, 2001). Implicitly, we assume that the movements and pauses of those filaments were all on track. The filaments were tracked for an average of 2.26 min at 4- or 5-s time intervals (average = 4.73 s), and the total number of time intervals for all 72 filaments was 2061. For

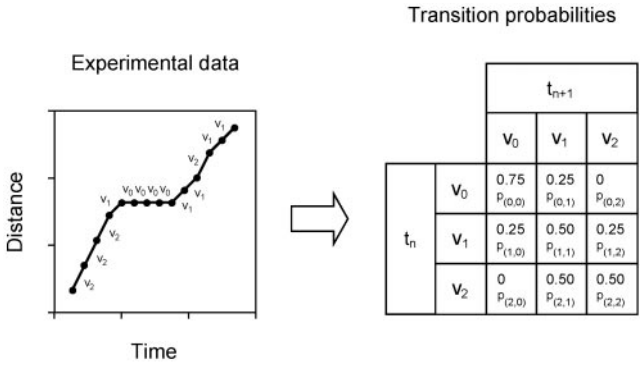

Figure 2. Schematic diagram illustrating the method for calculating the transition probabilities. For each neurofilament, we calculate a speed for each successive time interval. To simplify the computation, we group these interval speeds into discrete speed bins and then compute the frequency with which movement at a certain speed is followed by movement at the same speed and at each of the other speeds. The result is a matrix of transition probabilities. (A) A simplified hypothetical example of a single neurofilament in which there are three possible interval speed bins: v_0 (pausing), v_1, and v_2. (B) A matrix of transition probabilities calculated from the hypothetical data in A. Each transition probability, $p_{(i,j)}$, represents the probability that a neurofilament moving at speed v_i in time interval, t_n, will move at speed v_j in the subsequent time interval, t_{n+1}.

each time interval we calculated an interval speed, which we define as the distance moved in one time interval divided by the duration of one time interval. Because we found no evidence for a relationship between the speed or pausing behavior and the direction of movement (Wang *et al.*, 2000; Wang and Brown, 2001), we pooled the data for anterograde and retrograde movements. Movements of ≤ 0.065 μm/s (1 camera pixel per second), which we estimated to be the limit of the precision of our measurements, were defined as pauses. Using this approach, we obtained a total of 1989 interval speeds. To simplify the computation, we assigned each interval speed to one of seven speed bins: v_0: $v = 0$ (i.e., pausing); v_1: $0 < v \leq 0.5$ μm/s; v_2: $0.5 < v \leq 1.0$ μm/s; v_3: $1.0 < v \leq 1.5$ μm/s; v_4: $1.5 < v \leq 2.0$ μm/s; v_5: $2.0 < v \leq 2.5$ μm/s; and v_6: $2.5 < v \leq 3.0$ μm/s.

To calculate the probability of switching between these speed bins, we counted the number of times that a filament moving in speed bin v_i moved in speed bin v_j in the subsequent time interval, as shown schematically in Figure 2. For each value of i, the number of transitions from v_i to v_j was expressed as a fraction of the total number of transitions from that value of i to all values of j. The result was a matrix of 49 transition probabilities, p(i, j) (Table 1). Generally speaking, it can be seen that the probability of pausing is higher for filaments that are already pausing and lower for filaments that are moving rapidly and the probability of moving rapidly is higher for filaments that are already moving rapidly and lower for filaments that are pausing.

The Algorithm

To simulate the movement of neurofilaments, we start with a specified number of neurofilaments distributed along the axon in a specified manner and then determine their position and velocity iteratively for a specified number of time intervals (Figure 3). We use a time interval of 4.73 s, which represents the average time interval used in our experimental studies (see above). We consider the location of each neurofilament to be a single point in space that might be considered the middle of the filament. This is a reasonable assumption given that the average length of neurofilament polymers is small relative to the segment length (3 mm) and axon length (several centimeters) in the radioisotopic pulse-labeling experiments (see below). For simplicity, we assume that neurofilaments can switch on and off track and between anterograde and retrograde states only when they are pausing. If the filament is moving, we generate a pseudorandom number within the range 0–1 and compare it to the probabilities in the matrix of transition probabilities in Table 1 to determine whether the filament remains in the same speed bin or switches to a new speed bin. Then we use the new speed to calculate a new location for the filament. If the filament is pausing, we generate a pseudorandom number to determine its directional state (governed by the probabilities p_A and p_R) and a second pseudorandom number to determine whether the filament is on or off track (governed by the probabilities p_{ON} and p_{OFF}). For filaments that are on track, we then determine a new location for the filament based on the new direction and speed as described above. Pseudorandom numbers are generated using the ran2 algorithm (Press *et al.*, 1992).

Table 1. Transition probabilities for neurofilament movement

		t_{n+1}							
		v_0 (pause)	v_1	v_2	v_3	v_4	v_5	v_6	n
t_n	v_0 (pause)	0.856 $p_{(0,0)}$	0.112 $p_{(0,1)}$	0.029 $p_{(0,2)}$	0.002 $p_{(0,3)}$	0.001 $p_{(0,4)}$	0.001 $p_{(0,5)}$	0.000 $p_{(0,6)}$	1294
	v_1	0.440 $p_{(1,0)}$	0.385 $p_{(1,1)}$	0.115 $p_{(1,2)}$	0.052 $p_{(1,3)}$	0.006 $p_{(1,4)}$	0.000 $p_{(1,5)}$	0.003 $p_{(1,6)}$	364
	v_2	0.236 $p_{(2,0)}$	0.311 $p_{(2,1)}$	0.298 $p_{(2,2)}$	0.130 $p_{(2,3)}$	0.019 $p_{(2,4)}$	0.000 $p_{(2,5)}$	0.006 $p_{(2,6)}$	161
	v_3	0.092 $p_{(3,0)}$	0.197 $p_{(3,1)}$	0.263 $p_{(3,2)}$	0.382 $p_{(3,3)}$	0.053 $p_{(3,4)}$	0.013 $p_{(3,5)}$	0.000 $p_{(3,6)}$	76
	v_4	0.133 $p_{(4,0)}$	0.267 $p_{(4,1)}$	0.267 $p_{(4,2)}$	0.267 $p_{(4,3)}$	0.067 $p_{(4,4)}$	0.000 $p_{(4,5)}$	0.000 $p_{(4,6)}$	15
	v_5	0.000 $p_{(5,0)}$	0.200 $p_{(5,1)}$	0.200 $p_{(5,2)}$	0.400 $p_{(5,3)}$	0.200 $p_{(5,4)}$	0.000 $p_{(5,5)}$	0.000 $p_{(5,6)}$	5
	v_6	0.000 $p_{(6,0)}$	0.000 $p_{(6,1)}$	0.000 $p_{(6,2)}$	0.500 $p_{(6,3)}$	0.000 $p_{(6,4)}$	0.500 $p_{(6,5)}$	0.000 $p_{(6,6)}$	2

This table shows a matrix of 49 transition probabilities calculated from our experimental data on the movement of neurofilaments through photobleached gaps in the axonal neurofilament array of cultured rat sympathetic neurons (Wang and Brown, 2001). The total number of filaments tracked was 72 and the time-lapse intervals were 4 or 5 s (average = 4.73 s). The interval speeds for anterograde and retrograde filaments were pooled and then binned into seven categories: v_0 ($v = 0$ μm/s), v_1 ($0 < v \leq 0.5$ μm/s), v_2 ($0.5 < v \leq 1.0$ μm/s), v_3 ($1.0 < v \leq 1.5$ μm/s), v_4 ($1.5 < v \leq 2.0$ μm/s), v_5 ($2.0 < v \leq 2.5$ μm/s), and v_6 ($2.5 < v \leq 3.0$ μm/s). Each transition probability $p_{(i,j)}$ represents the probability that a neurofilament moving at speed v_i in time interval, t_n, will move at speed v_j in the subsequent time interval, t_{n+1}. For each element of the matrix, the number of transitions $v_i \rightarrow v_j$ is expressed as a fraction of the total number of transitions $v_i \rightarrow v_j$ for all values of j (shown in the column labeled n). The total number of transitions was 1917.

RESULTS

Initial Estimation of the Parameters of the Model

Our observations in cultured neurons indicate that 31% of the neurofilaments move retrogradely and 69% move anterogradely (Wang and Brown, 2001), so we assume that $p_R = 0.31$ and $p_A = 0.69$. The rates k_{REV}, k_{ON}, and k_{OFF} are unknown, so we initially estimated the values of these parameters and subsequently optimized them as described below. In two separate studies on neurofilament movement in cultured neurons, we observed a total of 141 filaments for a total observation time of 5.4 h (4111 time intervals), yet we observed no sustained reversals (Wang *et al.*, 2000; Wang and Brown, 2001). In another study, Roy *et al.* (2000) reported 5 of 73 neurofilaments reversed direction, but some of those neurofilaments exhibited unusually erratic behavior, reversing multiple times within the short period of time that they were tracked. Thus the magnitude of k_{REV} is low. As a starting point for our simulations, we assume $k_{REV} = 0.001$ ($k_{AR} = 0.00031$ and $k_{RA} = 0.00069$). Because the existence of distinct on-track and off-track populations of neurofilaments is hypothetical, we have no experimental data to guide our selection of values for k_{ON} and k_{OFF}. However, we expect that filaments must spend most of their time off track to account for the overall slow rate of movement. As a starting point for our simulations, we assume $k_{ON} = 0.01$ and $k_{OFF} = 0.1$ (~9% of neurofilaments on track).

Simulation of the Movement of a Single Neurofilament

To test the model, we first simulated the movement of a single neurofilament (Figure 4). At the start of the simulation, we consider the filament to be off track in the anterograde state. Figure 4, A–E, shows representative excerpts of the simulated behavior of a single neurofilament, including both anterograde and retrograde phases of its movement, assuming $k_{ON} = 0.01$, $k_{OFF} = 0.1$, and $k_{REV} = 0.001$. The filament exhibited brief bouts of rapid movement interrupted by pauses of varying duration. Consistent with our experimental data, the transitions between movements and pauses were abrupt and reversals were rare; in a 24-h simulation the filament reversed direction eight times, which represents a frequency of 0.00044 per time interval, consistent with the theoretical prediction $p_A k_{AR} + p_R k_{RA}$. Figure 4, F–J, shows representative plots of actual neurofilament behavior observed by time-lapse fluorescence microscopy in cultured neurons (data from the study of Wang and Brown, 2001). It can be seen that the model generates a motile behavior very similar to the experimental data, except that some of the pauses in the simulation are much longer. This is expected because our model assumes that filaments can enter an off-track state in which they pause for prolonged periods (as explained in *Materials and Methods*, our experimental studies were biased toward the detection of moving filaments; filaments that did not move during the time that we observed them could not be tracked and therefore were excluded from our analyses).

Analysis of the Pause Durations

In a stochastic system characterized by alternating movements and pauses, we can gain insight into the mechanism of movement by analyzing the frequency distribution of the pause durations. Specifically, if we consider that there is no off-track state and we define the rate at which neurofilaments transition from the pausing state to a moving state as k_{PM}, then a histogram of the pause durations will be exponentially distributed proportional to $\exp(-k_{PM}t)$, and the exponential will decrease with a time constant $1/k_{PM}$ (Van Kampen, 1981). If we now consider distinct on-track and off-track states, with transitions between them dictated by k_{ON} and k_{OFF}, then we expect to observe the superimposi-

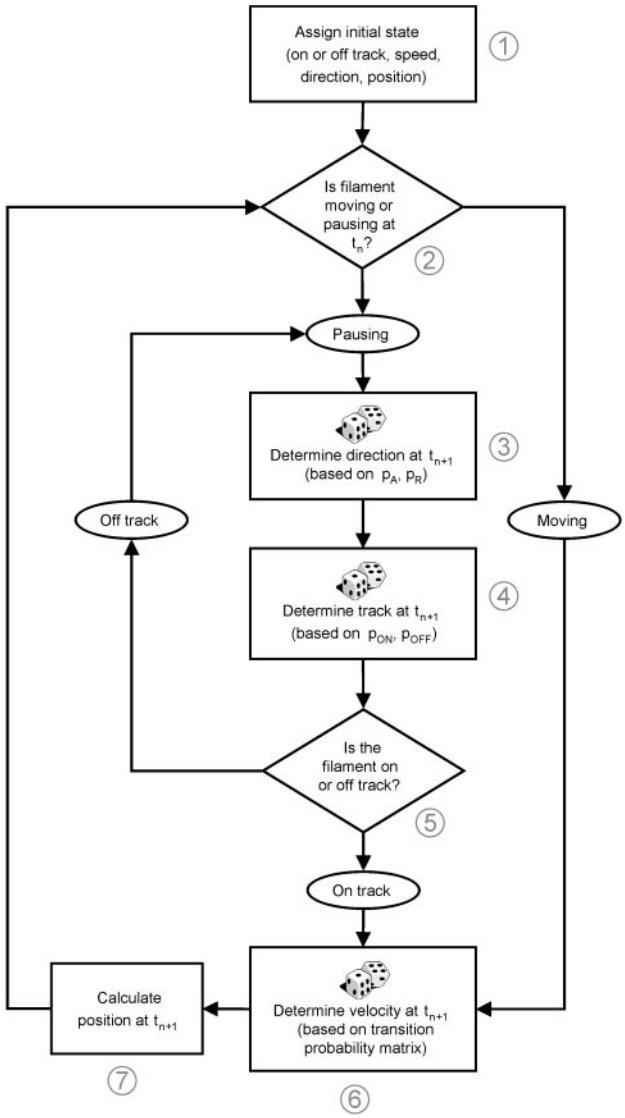

Figure 3. Flowchart showing the algorithm used for the simulations. At the start of each simulations, each filament is assigned to be either on or off track and either anterograde or retrograde and each filament is also assigned a speed and a position along the axon (1). Each time interval (t_n), we determine whether the filament is currently moving or pausing (2). If the filament is currently moving, then we determine a new velocity for the next time interval (t_{n+1}) based on the transition probability matrix (6) and then we calculate a new position (7). If the filament is currently pausing, then we determine whether it will now change its directional state based on the probabilities p_A and p_R (3) and whether it will now be on or off track based on the probabilities p_{ON} and p_{OFF} (4). The next action depends on whether the filament is now on track or off track (5). If the filament is now on track, then we determine a new velocity based on the transition probability matrix (6) and then calculate a new position (7). Alternatively, if the filament is now off track, then it must remain paused. The flow chart loops once each time interval. The diamond boxes represent decision points where the flow chart branches and the square boxes represent calculations or assignment of values. The symbol of the pair of dice indicates a point in the algorithm in which the outcome is determined by a random number generator.

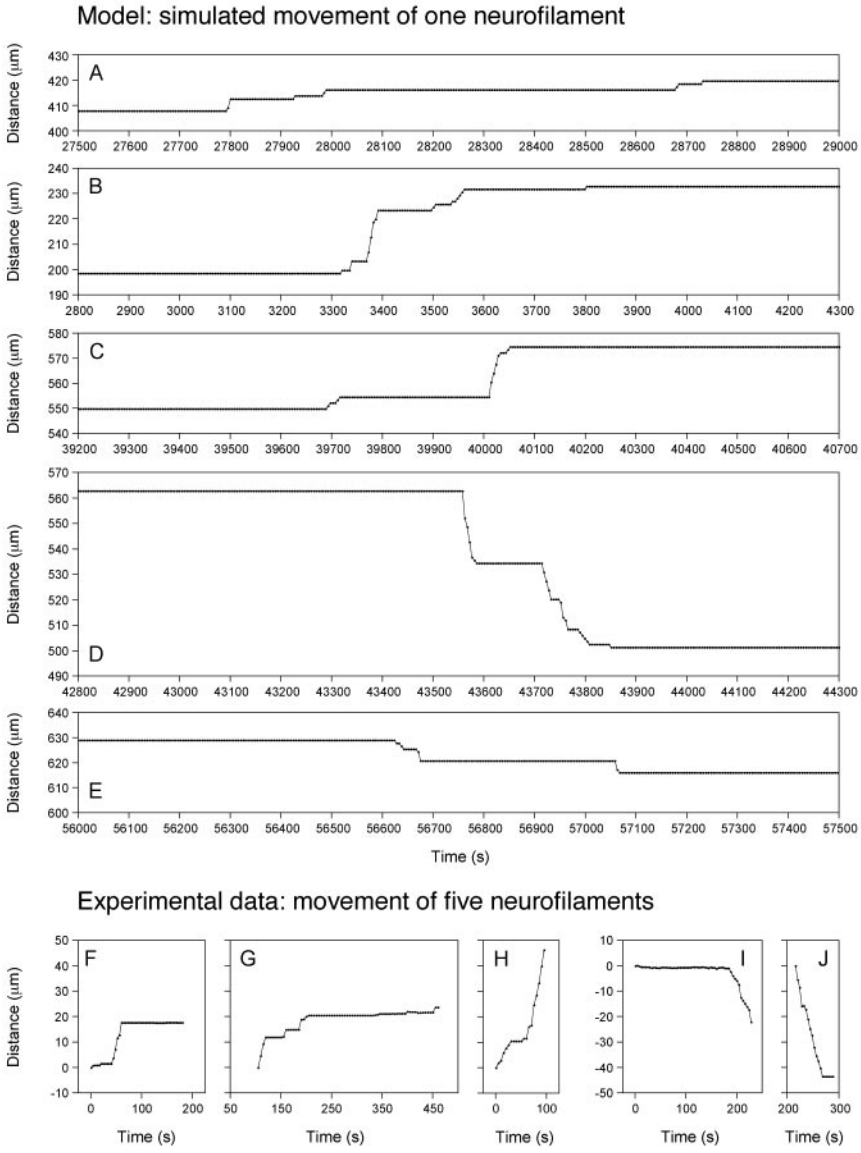

Figure 4. Comparison of simulated and actual behavior of single neurofilaments. (A–E) Simulated movement of a single neurofilament along an axon, assuming k_{ON} = 0.01, k_{OFF} = 0.1, and k_{REV} = 0.001. The filament was in the anterograde state and pausing off track at the start of the simulation. Each graph represents a different 1500-s portion of the simulation, illustrating both anterograde (A–C) and retrograde (D and E) phases of the movement. The filament exhibited brief bouts of rapid movement interrupted by pauses of varying duration. (F–J) Actual experimental data on the movement of five neurofilaments in axons of cultured neurons observed by fluorescence photobleaching (from the study of Wang and Brown, 2001). Examples of anterograde (F–H) and retrograde (I and J) movements are shown. Note that these filaments could only be tracked for short periods because of the narrow observation window and short movie duration inherent in our live cell imaging studies (see text). The transitions between different speeds are more discrete in the simulation than in the actual data because the speeds have been binned. Note that the motile behavior is very similar, except that some of the pauses in the model are more prolonged.

tion of two exponentials with time constants of $1/k_{PM}$ and $1/k_{ON}$. Figure 5A shows the pause duration frequency distribution generated by our model, assuming k_{ON} = 0.01, k_{OFF} = 0.1, and k_{REV} = 0.001. As expected, the distribution is biphasic and matches a double exponential relationship due to the existence of distinct on-track and off-track states for the neurofilaments. The initial (rapidly declining) phase of these plots is due primarily to on-track pauses (shorter duration) and the later (slowly declining) phase is due primarily to off-track pauses (longer duration). Figure 5, B and

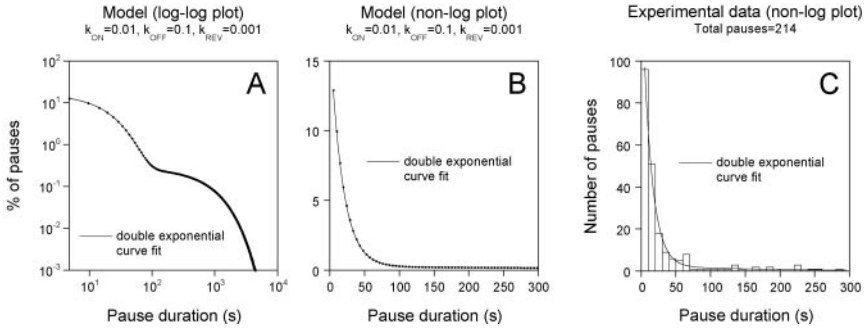

Figure 5. Comparison of simulated and actual pause duration frequency distributions. (A and B) Pause duration frequency distribution generated by the model, assuming k_{ON} = 0.01, k_{OFF} = 0.1, and k_{REV} = 0.001, plotted as a log-log plot in A and as a nonlog plot in B. (C) Actual pause duration frequency distribution obtained experimentally for neurofilaments in axons of cultured neurons (previously unpublished data from the study of Wang and Brown, 2001). The distribution in C is unreliable at longer pause durations due to the short duration of our movies and our inability to track neurofilaments that paused throughout the observation period (see *Materials and Methods*). The curves represent the best fit to a double exponential function.

C, shows the frequency distribution of the actual pause durations for neurofilaments in cultured neurons (previously unpublished data from the study of Wang and Brown, 2001). Note that the shape of the predicted distribution is similar to that of the experimental data (compare Figure 5, B and C). However, we consider that the experimental data in Figure 5C is only reliable for short pauses because our experimental observations underestimate the number and duration of long pauses (see *Materials and Methods*). Because the frequency distribution for short pause durations can be characterized by its initial slope, we define the initial slope of the histogram in Figure 5C as the benchmark for optimization of the pause distributions in our model (see below).

Simulation of the Movement of a Population of Neurofilaments

To investigate the behavior of the model in a radioisotopic pulse-labeling experiment, we first simulated the movement of a population of radiolabeled neurofilaments distributed uniformly along a 3-mm length of axon (i.e., in the form of a 3-mm-wide square wave; Figure 6 and Supplementary Video, QuickTime Movie 1). At the start of each simulation, we considered all filaments to be off track and 31% to be in the retrograde state. Note, however, that these starting conditions have no significant effect on the end result because of the long duration of the simulations (several weeks) relative to the short duration of the time intervals. We found that the square wave spreads rapidly to form a Gaussian wave that continues to spread as it propagates distally, as generally expected for a stochastic process (for the specific conditions under which this applies, see Jung *et al.*, 1996). Notably, the shape and spreading of this wave is similar to the behavior described for neurofilaments in vivo (e.g., Hoffman *et al.*, 1985; Jung and Shea, 1999; Xu and Tung, 2000).

To characterize the model further, we investigated the effect of k_{ON}, k_{OFF}, and k_{REV} on the transport kinetics (Figure 7). To avoid artifacts associated with the initial transition from a square wave to a Gaussian wave, we used a Gaussian wave as the starting point for each simulation. We then ran multiple simulations and systematically varied three parameters: the ratio k_{ON}/k_{OFF}, keeping the magnitude of k_{OFF} constant (Figure 7, A–C); the magnitudes of k_{ON} and k_{OFF}, keeping the ratio k_{ON}/k_{OFF} constant (Figure 7, D–F); and the magnitude of $k_{REV} = k_{RA} + k_{AR}$, keeping the ratio k_{AR}/k_{RA} constant (Figure 7, G–I). As expected, for all conditions tested, the wave propagates anterogradely at a constant rate. We found that varying the ratio k_{ON}/k_{OFF} while keeping k_{OFF} constant affects both the average velocity (Figure 7A) and the spreading of the wave (Figure 7B), whereas varying k_{ON} and k_{OFF} while keeping the ratio k_{ON}/k_{OFF} constant does not affect the average velocity (Figure 7D) but does affect the spreading (Figure 7E). Varying k_{REV} has no effect on the average velocity (Figure 7G), but does affect the spreading (Figure 7H).

Figure 7, C, F, and I, shows the effects of varying k_{ON}, k_{OFF}, and k_{REV} on the pause durations. The curves are biphasic, as described above, but the inflection between the two phases of the curves increases with decreasing k_{ON}/k_{OFF} ratio, keeping the magnitude of k_{OFF} constant (Figure 7C) and also with decreasing magnitudes of k_{ON} and k_{OFF}, keeping the k_{ON}/k_{OFF} ratio constant (Figure 7F). Varying the k_{ON}/k_{OFF} ratio while keeping k_{OFF} constant has no effect on the initial slope of the pause duration frequency distribution (primarily on-track pauses), but does have a marked effect on the distribution for longer pause durations (Figure 7C), whereas varying the magnitude of k_{ON} and k_{OFF} while keeping the ratio constant affects the distribution of both short and long pause durations (Figure 7F). Varying k_{REV} has no effect on the pause durations (Figure 7I)

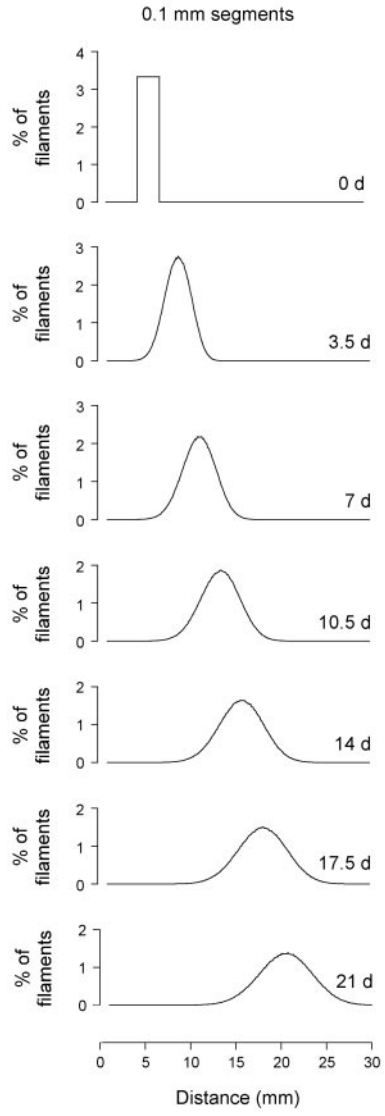

Figure 6. The model produces a Gaussian wave. Simulated movement of a pulse of 1,000,000 radiolabeled neurofilaments along a nerve for 21 d starting with a 3-mm-wide square wave and assuming $k_{ON} = 0.01$, $k_{OFF} = 0.1$, and $k_{REV} = 0.001$. The positions of the neurofilaments were binned into 0.1-mm segments at 0.5-d intervals. The square wave adopts a Gaussian wave form as the neurofilaments move along the axon, reminiscent of the bell-shaped waves observed in radioisotopic pulse-labeling experiments. See Supplementary Video QuickTime Movie 1.

In summary, the only parameter that affects the average rate of movement is the ratio k_{ON}/k_{OFF} (Figure 7A). Both the ratio k_{ON}/k_{OFF} and the magnitudes of k_{ON} and k_{OFF} affect the pause duration distribution (Figure 7, C and F), but the only parameters that affect the initial slope are the magnitudes of k_{ON} and k_{OFF}. (Figure 7F). All three parameters affect the spreading of the wave, but only k_{REV} does so without affecting the pause duration frequency distribution

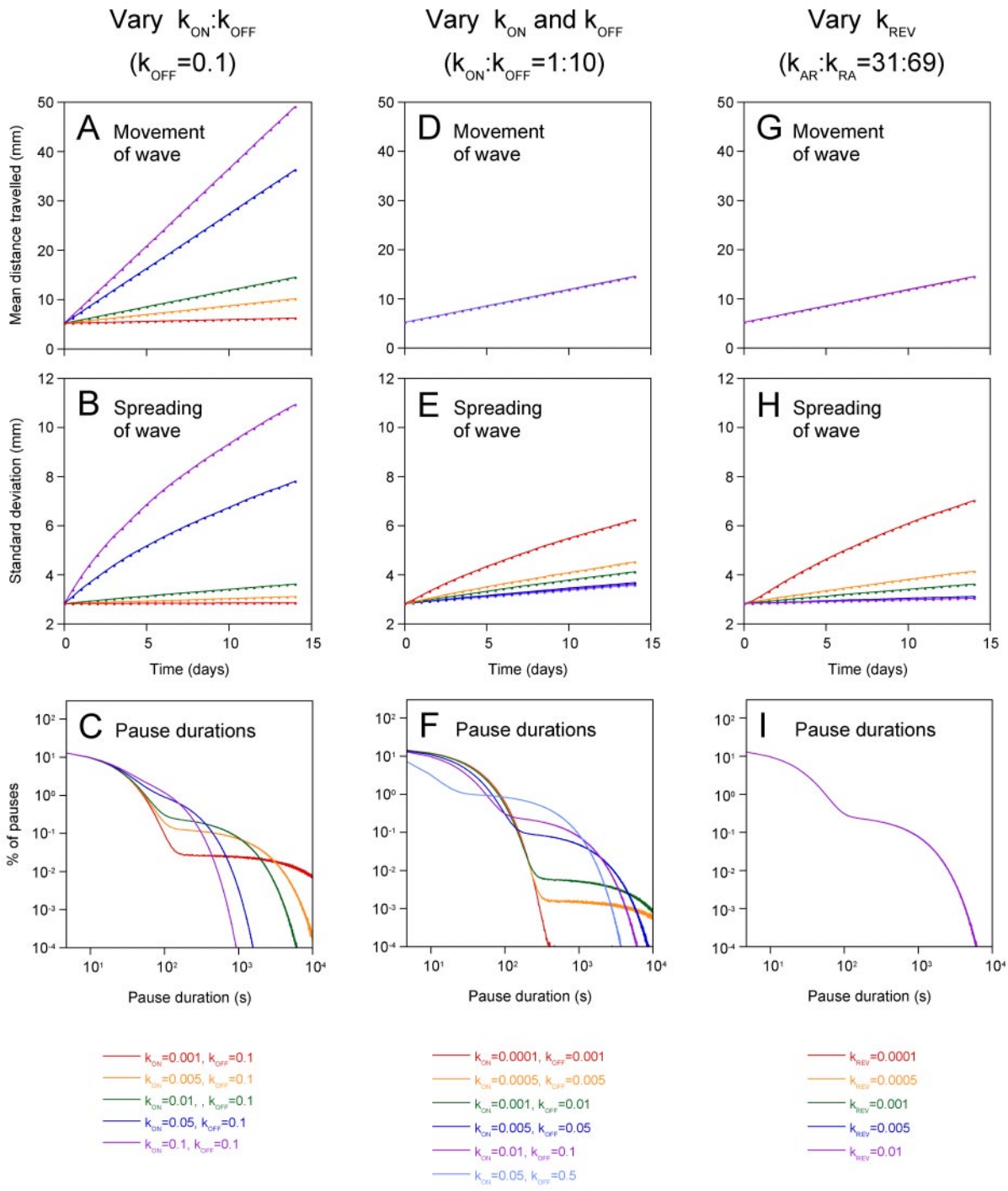

Figure 7. Effect of k_{ON}, k_{OFF}, and k_{REV} on the velocity, spreading, and pause duration frequency distribution of the neurofilament population in a simulated pulse-labeling experiment. All simulations were performed with 20,000 neurofilaments for a period of 14 d, starting with the neurofilaments distributed in a Gaussian waveform optimized to match the experimental data of Xu and Tung (2000) at day 7 (see Figure 8). (A–C) Effect of varying the ratio k_{ON}/k_{OFF}, keeping k_{OFF} = 0.1. (D–F) Effect of varying k_{ON} and k_{OFF}, keeping the ratio k_{ON}/k_{OFF} = 1/10. (G–I) Effect of varying the rate of reversal, $k_{REV} = k_{AR} + k_{RA}$, keeping k_{AR}/k_{RA} = 31/69. (A, D, and G) The average distance moved by the neurofilaments as a function of time. (B, E, and H) The width of the wave (expressed as the SD of the Gaussian wave) as a function of time. (C, F, and I) The pause duration frequency distributions for the neurofilaments summated over the entire simulation (log-log plots).

(Figure 7I). Thus, any given combination of average rate, spreading, and pause duration frequency distribution in this model corresponds to a single unique combination of values for the parameters k_{ON}, k_{OFF}, and k_{REV}.

Optimization of the Parameters to Match the In Vivo Data

To test whether the model can explain the kinetics of neurofilament transport in vivo, we examined whether it can

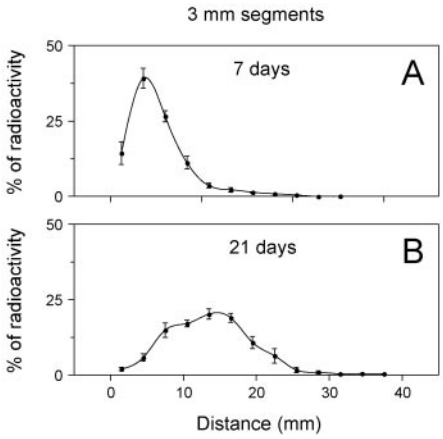

Figure 8. Experimental radioisotopic pulse-labeling data for neurofilament protein L in mouse ventral root and sciatic nerve, provided by Zuoshang Xu (Xu and Tung, 2000). The segment length was 3 mm. The data are normalized to the total amount of radioactive neurofilament protein L in the nerve and plotted as a function of distance from the spinal cord. (A) 7 d after isotope injection. (B) Twenty-one days after isotope injection. Each point is the mean of three to five nerves. The error bars represent the SE of the mean (SEM). The curves were drawn using a cubic spline curve-fitting algorithm. Note that there is considerable statistical error associated with radioisotopic pulse-labeling data because each point is the average of data from multiple animals, each of which corresponds to a separate isotope injection. The hump to the left of the peak in the experimental data at 21 d is an example of this statistical variability; it is not a consistent feature of the neurofilament transport kinetics in these nerves (Xu and Tung, 2000, 2001).

match the shape, rate, and spreading of the wave for a real set of pulse-labeling data, while at the same time matching the initial slope of the pause duration frequency distribution. Because it is not possible to measure the pause durations of neurofilaments experimentally in vivo, we used our data from cultured neurons (Figure 5C). We chose to model the radioisotopic pulse-labeling data of Xu and Tung (2000) for neurofilament protein L in ventral root and sciatic nerve motor axons of wild-type mice because this is one of the few published data sets for which the statistical error has been calculated for each data point (Figure 8). In the Xu and Tung study, the average velocity of neurofilament transport was found to be approximately constant during the first 3 wk and then slowed at later times, indicating that the velocity of neurofilament transport varies along the length of these axons (see *Discussion*). For the purposes of this study, we chose to focus on the initial 3-wk period when the velocity is constant. Because the exact length, duration, and shape of the starting pulse in the pulse-labeling experiments is not known, we started our simulations with a distribution of neurofilaments that matches the day 7 data (Figure 8A), at which time most of the filaments had entered the ventral root, and then attempted to match the distribution of neurofilaments at day 21, 2 wk later (Figure 8B).

Figure 9 shows the results of our simulations of the Xu and Tung data. For ease of computation, we fit the day 7 data using a Gaussian function and used this Gaussian curve as the starting distribution for our simulations (Figure 9A). Note that the Gaussian curve matches the experimental data closely, though there is a slight discrepancy at the leading edge. Using our initial "best guess" values for the model parameters ($k_{ON} = 0.01$, $k_{OFF} = 0.1$, $k_{REV} = 0.001$), we found that the simulated neurofilament population moved too fast and did not spread enough compared with the experimental data (Figure 9B). In addition, the initial slope of the pause duration frequency distribution did not match the experimental data (Figure 9G). We have shown above that the only parameter or combination of parameters that affects average velocity in our model is the ratio k_{ON}/k_{OFF} (Figure 7). By decreasing k_{ON}/k_{OFF} to 0.0083, we were able to match the average velocity of the experimental data (Figure 9C). This had little effect on width of the wave because the ratio k_{ON}/k_{OFF} has little effect on spreading at low ratios (Figure 7B). As expected, based our earlier findings (Figure 7C), changing k_{ON}/k_{OFF} had no effect on the initial slope of the pause duration frequency histogram (Figure 9H).

We have shown above that the only parameters in our model that affect the initial slope of the pause duration frequency histogram are the magnitudes of k_{ON} and k_{OFF}. By increasing the magnitudes of k_{ON} and k_{OFF} to 0.0175/0.211, keeping the ratio constant, we were able to match the initial slope of the pause duration frequency histogram (Figure 9I). As expected, based on our earlier findings (Figure 7D), this had no effect on the average velocity (Figure 9D). Finally, we were able to match the spreading of the wave by decreasing k_{REV} to 0.00012 (Figure 9E). As expected, based on our earlier findings (Figure 7, G and I), this had no effect on the average velocity or the pause durations. Thus we are able to match the experimental data with a particular combination of values for the parameters k_{ON}, k_{OFF}, and k_{REV} and this is a unique solution under the constraints of our model; no other combination of these parameters can match the data.

Because the existence of distinct on-track and off-track populations of neurofilaments is hypothetical, we examined whether we could match the experimental data if we assumed that all neurofilaments are on track (this is the equivalent of assuming $k_{OFF} = 0$ in our model). As expected, we found that the pulse of radiolabeled neurofilaments moved too fast and the wave spread too little (data not shown). The spreading could be increased by decreasing k_{REV}, but this had no effect on the velocity because the only way to affect average velocity in our model is to alter the ratio k_{ON}/k_{OFF} (Figure 7G). We also examined whether we could match the experimental data if we assumed that neurofilaments can only move anterogradely (this is the equivalent of assuming $k_{AR} = 0$ and $k_{RA} = 1$ in our model). Under this condition, the wave moved too fast and spread too little, and there was no combination of k_{ON} and k_{OFF} that could match the experimental data (data not shown). Thus our model cannot match the in vivo experimental data unless we assume that there are distinct on-track and off-track populations of neurofilaments in vivo and that neurofilament transport is bidirectional in vivo.

Figure 10 and Supplementary Video QuickTime Movie 2 show a simulated radioisotopic pulse-labeling experiment using the final optimized parameters obtained above, and Figure 11 shows the average velocity, spreading, and pause duration frequency distribution for this simulation. Supplementary Video QuickTime Movie 3 is a graphic representation of the simulated behavior for 22 neurofilaments in a 200-μm segment of axon over a period of 1 h. Because the plots in Figure 11 represent the result of our optimized simulation, they can be considered to be predictions of neurofilament behavior in vivo. The average distance moved was linear with respect to time, with an average velocity of 0.56 mm/d (Figure 11A). The spreading of the wave increased in a nonlinear manner (Figure 11B) and was proportional to $t^{1/2}$ when the simulation was extended to longer times (data not shown). Based on the optimized values of the

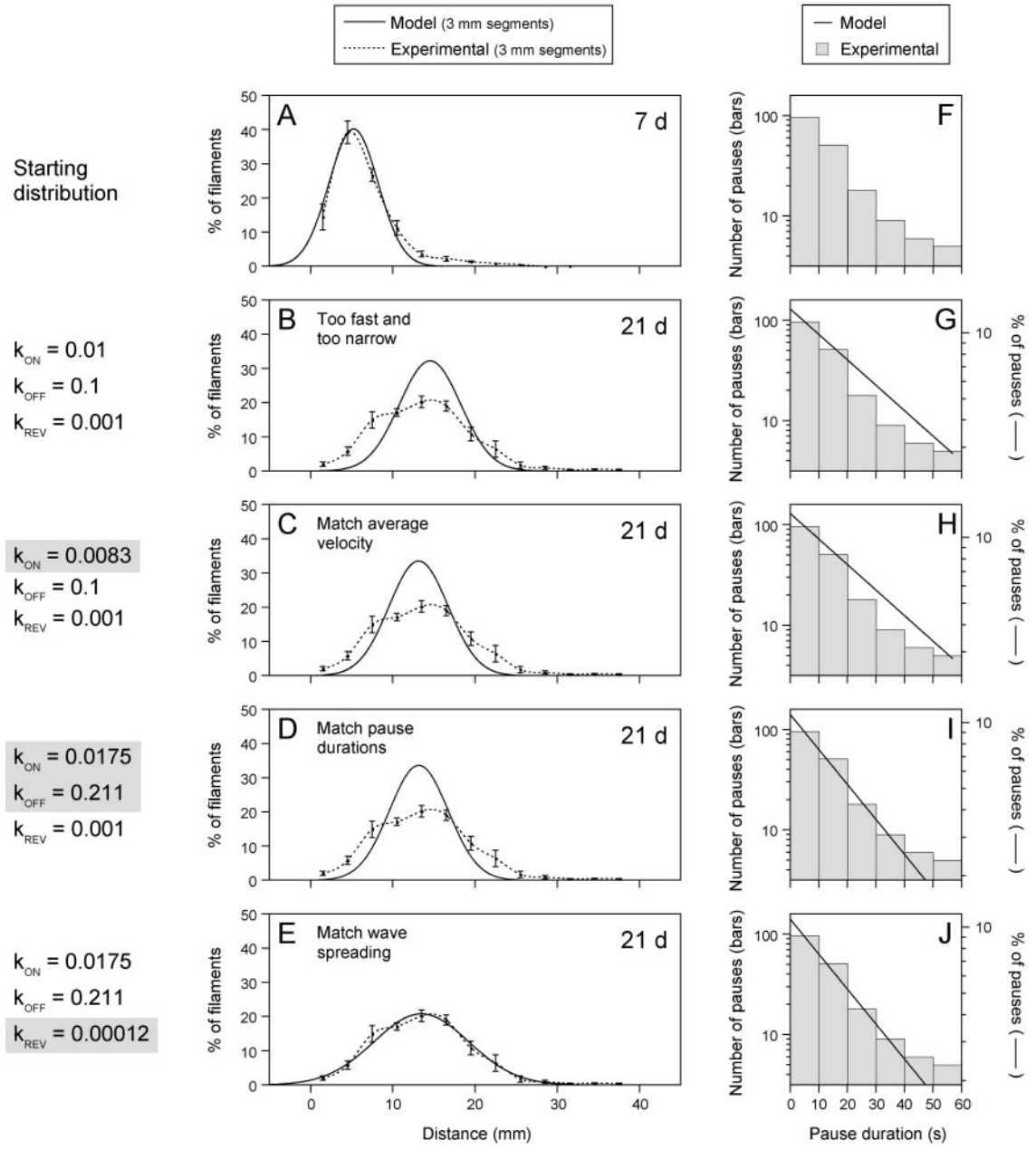

Figure 9. Optimization of the model to match the experimental data. We systematically varied the parameters k_{ON}, k_{OFF}, and k_{REV} in order to match the model to the experimental radioisotopic pulse-labeling data of Xu and Tung (2000). All simulations were performed with 20,000 neurofilaments for a period of 14 d, starting with the neurofilaments distributed in a Gaussian waveform that closely matches the experimental data at day 7 (see Figure 8). The positions of the neurofilaments generated by the model were binned into 3-mm segments and fitted with a Gaussian curve. The optimization of the rate and spreading of the wave is shown in A–E. The dashed lines represent the experimental data for neurofilament protein L in mouse ventral root and sciatic nerve and the solid lines represent the simulated data. The optimization of the initial slope of the pause duration frequency distribution is shown in F–J (semilog plots). The bars represent the experimental pause duration frequency distribution (for durations <60 s; data from Figure 5C) and the solid lines represent the initial slope of the pause duration frequency distribution for the model. (A) Experimental data at day 7, and the corresponding Gaussian curve fit. (B–E) Comparison of the experimental and simulated transport waves at 21 d after injection. (F–J) Comparison of the experimental and simulated pause duration frequency distributions at 21 d after injection. The values of the parameters k_{ON}, k_{OFF}, and k_{REV} used for the simulations are indicated to the left of the plots. Using our initial "best guess" values for the parameters, the wave moves too fast and does not spread enough (B) and the initial slope of the pause duration frequency distribution does not match the experimental data (G). Reducing the ratio k_{ON}/k_{OFF} reduces the average velocity (C) but does not affect the pause duration frequency distribution (H). Increasing k_{ON} and k_{OFF}, keeping the ratio k_{ON}/k_{OFF} constant has little effect on the wave (D), but reduces the initial slope of the pause duration frequency distribution (I). Finally, reducing k_{REV} increases the spreading (E) without affecting the pause durations (J). The resulting simulated wave is statistically indistinguishable from the experimental data ($p < 0.005$, Kolmogorov-Smirnov test for goodness of fit). Thus the model can match the experimental data, assuming $k_{ON} = 0.0175$, $k_{OFF} = 0.211$, and $k_{REV} = 0.00012$.

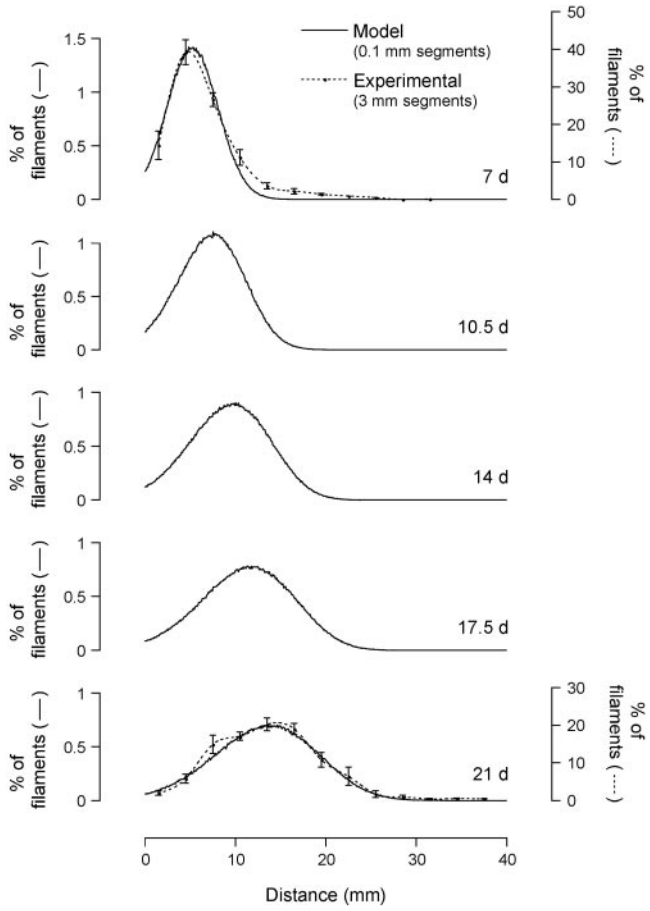

Figure 10. Optimized simulation of neurofilament protein transport in vivo. Final simulation for a pulse of 1,000,000 radio-labeled neurofilaments starting with a Gaussian wave that approximates the experimental data of Xu and Tung (2000) at day 7 and using the optimized parameters obtained from Figure 9 (k_{ON} = 0.0175, k_{OFF} = 0.211, and k_{REV} = 0.00012). The positions of the neurofilaments were binned into 0.1-mm segments and sampled at 0.5-d intervals. The wave maintains its Gaussian shape but spreads as it moves distally, closely matching the experimental data at day 21. See Supplementary Video QuickTime Movie 2.

parameters k_{ON} and k_{OFF}, the average proportion of the neurofilaments that was on track at any point in time was 8.0%. This number is slightly larger than $k_{ON}/(k_{ON} + k_{OFF})$ = 0.077 (i.e., 7.7% on track) because we assume that a filament cannot switch off track while it is moving. The average duration of continuous uninterrupted pausing was 430 s, but the range was large. For example, ~38% of the pauses were 1 min or less in duration and 16% of the pauses were 15 min or more in duration (Figure 11C). Moreover, the average duration of sustained uninterrupted movement was only 14 s. Thus movements were brief and pauses were prolonged. On average, the filaments spent 97% of their time pausing.

DISCUSSION

Validation of the Stop-and-Go Hypothesis

We have described a stochastic model of neurofilament movement in axons based on a detailed analysis of the moving and pausing behavior of neurofilaments in cultured nerve cells. The key features of our model are that neurofilaments move in both anterograde and retrograde directions along cytoskeletal tracks, alternating between short bouts of rapid movement and short pauses, and that they can temporarily disengage from these tracks, resulting in more prolonged pauses. To test our model, we simulated a radioisotopic pulse-labeling experiment in mouse ventral root and sciatic nerve. We show that the model generates a Gaussian waveform that is very similar to the waves observed in vivo. By systematically varying the parameters of the model, we obtained a single unique solution that could match the shape, rate, and spreading of the radiolabeled neurofilaments. Thus the moving and pausing behavior of neurofilaments observed by live cell fluorescence imaging in cultured nerve cells can explain the kinetics of slow axonal transport in vivo, which is a central tenet of the stop-and-go hypothesis. On the basis of the optimized values of the parameters in the model, we can make several predictions concerning the mechanism of movement in the motor axons of mouse ventral root and sciatic nerve: first, that neurofilament movement is bidirectional; second, that the frequency of reversals is low; third, that neurofilaments spend ~8% of their time on track; and fourth, that neurofilaments spend 97% of the time pausing during their journey along these axons. These predictions are discussed in more detail below.

Neurofilament Transport Is Bidirectional In Vivo

The idea that slow axonal transport may be a bidirectional process was first proposed more than a decade ago by Griffin and colleagues, based on their analysis of the distribution of cytoskeletal proteins in transected peripheral nerves in *Ola* mice, which exhibit delayed Wallerian degeneration. These authors reported that neurofilament and other cytoskeletal proteins accumulated proximally as well as distally in the isolated nerve segments, implying that a proportion of cytoskeletal proteins move retrogradely in vivo (Watson *et al.*, 1993; Glass and Griffin, 1994). This conclusion is supported by studies on transgenic mice over-

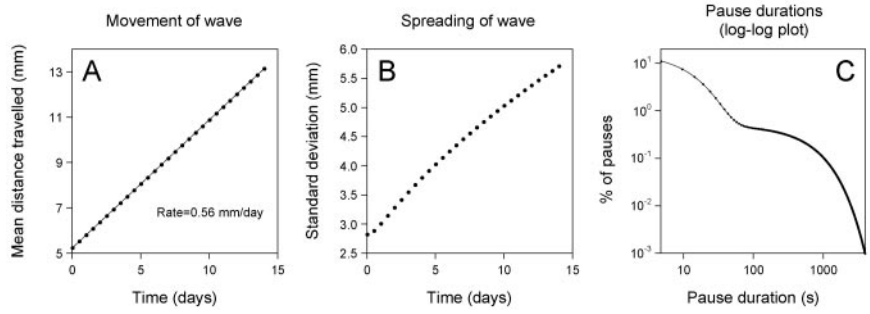

Figure 11. Analysis of neurofilament behavior for the optimized simulation shown in Figure 10. (A) Mean distance traveled plotted as a function of time. Note that the rate is constant (0.56 mm/d). (B) Width of wave (expressed as the SD) plotted as a function of time. (C) Pause duration frequency distribution. Note that the pause durations span a very wide range, from pauses as short as one time interval (4.73 s) to pauses in excess of several hours. On average, pauses were prolonged (average = 430 s), movements were brief (average = 14 s), and the filaments spent 97% of their time pausing.

expressing the p50/dynamitin subunit of dynactin. These mice develop a motor neuron disease characterized by accumulations of neurofilaments in axons, which implies that the activity of a retrograde microtubule motor is important for neurofilament transport along axons in vivo (LaMonte *et al.*, 2002). Our computational modeling studies lend further support to this notion. Specifically, we were unable to match the kinetics of neurofilament transport in mouse spinal motor neurons unless we assumed that neurofilaments move bidirectionally and that the frequency of reversals is low. In fact, these bidirectional excursions appear to be a significant contributor to the spreading of the wave.

Neurofilaments Can Pause for Prolonged Periods

Our model assumes that neurofilaments can exist in two states that differ in their pausing behavior. We refer to these states as on track and off track. Neurofilaments that are on track exhibit short bouts of rapid movement interrupted by short pauses, whereas neurofilaments that are off track are stationary for prolonged periods. In mouse lumbar spinal motor axons, we predict that neurofilaments spend 92% of their time pausing off track as they move along the axon. The idea that axonal neurofilaments spend a significant proportion of their time in a stationary state was originally proposed by Nixon and Logvinenko (1986) based on their analysis of the axonal transport of radiolabeled neurofilament proteins in mouse optic nerve. The data in that study were subsequently disputed on technical grounds (Lasek *et al.*, 1992), sparking a vigorous debate. In essence, the principal issue has been whether the data in the original Nixon and Logvinenko study represent pure neurofilament transport kinetics or whether the kinetics were contaminated with cytosolic proteins that comigrate with neurofilament proteins when subjected to one-dimensional SDS-PAGE. Although this controversy remains unresolved, our modeling indicates that the basic idea that neurofilaments may be stationary for prolonged periods during their transit along axons does appear to be correct. In fact, our modeling predicts that neurofilaments in mouse lumbar spinal motor axons spend only 3% of the time moving.

Mechanistically, we consider that on track and off track neurofilaments could differ in some way that influences their capability for movement. One factor that may regulate the frequency of neurofilament movement is phosphorylation of neurofilament protein H (Ackerley *et al.*, 2003). The molecular mechanism of this effect is not known, though it is attractive to speculate that neurofilament phosphorylation might act by affecting the activity of neurofilament motors or their affinity for the neurofilament cargo. Although our model does not assume the identity of the tracks along which neurofilaments move, it is likely that they are microtubules. For example, neurofilaments have been shown to move along microtubule polymers in vitro (Shah *et al.*, 2000) and there is evidence that neurofilaments are transported by microtubule motors (see below). Neurofilaments have been shown to interact with myosin Va, which suggests that they may also be capable of moving along microfilaments, but a recent study in cultured neurons has shown that neurofilament movement can be abolished by depolymerizing microtubules but not by depolymerizing microfilaments (Francis *et al.*, 2005), which suggests that microtubules are the principal substrate. Assuming that microtubules are the tracks, it is interesting to note that in myelinated axons, which contribute more than 95% of the slowly transported radioactivity in the radioisotopic pulse-labeling studies (Wujek *et al.*, 1986), neurofilaments generally outnumber microtubules. For example, in the sciatic nerve of 14-wk-old mice, neurofilaments outnumber microtubules by 7:1 in small axons (<1.5 μm internodal diameter) and by 16:1 in large axons (>3.5 μm internodal diameter; Reles and Friede, 1991). In occulomotor nerve of 4-wk-old chickens, neurofilaments outnumber microtubules by 69:1 in somatic motor axons and 97:1 in parasympathetic axons (Price *et al.*, 1988). A consequence of this high axonal neurofilament:microtubule ratio is that at any given point in time many neurofilaments may not be adjacent to a microtubule. Thus one factor that may contribute to the distinct pausing behavior of neurofilaments in the on track and/or off track states is their proximity to the tracks along which they move.

The Significance of the Bell-shaped Waves

The bell-shaped waves characteristic of radioisotopic pulse-labeling studies on slow axonal transport were first described more than 25 years ago, yet remarkably little is known about how they are generated. In the present study, we show that the bell-shaped waves obtained for neurofilaments in mouse ventral root and sciatic nerve are approximately Gaussian and can be considered to represent the movement of a population of filaments at a broad range of rates, dictated largely by stochastic variation in the direction and frequency of movement. At any point in time those neurofilaments at the leading edge of the wave happened to have moved more frequently than others, or more consistently in an anterograde direction, whereas those at the trailing edge of the wave happened to have moved less frequently, or more frequently in a retrograde direction. Over time, the population spreads apart but the net direction is anterograde because on average the filaments spend more time moving anterogradely than retrogradely. According to this perspective, individual filaments can sustain rapid rates of movement for short periods of time, but all filaments eventually pause or reverse direction and thus the average velocity is slow. However, it should be noted that spreading Gaussian waves can be generated by a variety of different mechanisms, and thus they are certainly not unique to our model. In fact, similar kinetics were observed by Blum and Reed (1989) based on the assumption that neurofilament transport is a slow unidirectional movement. Thus the significance of our modeling is not so much that we can match the experimental data in vivo, but that we can do so with a model based actual experimental measurements of the stop-and-go motile behavior of neurofilaments in living cells.

Temporal and Spatial Variations in Neurofilament Transport Behavior

In this study, we showed that our model can match the kinetics of neurofilament transport in vivo when the average velocity of movement is constant. However, there are examples in the literature in which the average rate of neurofilament transport varies both spatially and temporally. For example, Xu and Tung (2000, 2001) have shown that rate of neurofilament transport in mouse lumbar ventral root and sciatic nerve decreases abruptly ~12–15 mm from the spinal cord, which corresponds to the point at which the motor axons emerge from the vertebral foramen. In addition, Hoffman and colleagues have reported a slowing of neurofilament transport with both developmental age and distance along the axons in lumbar ventral root and sciatic nerve of rats (Hoffman *et al.*, 1983, 1985). In our model of neurofilament transport, the average velocity of the wave of radiolabeled proteins is determined by the ratio k_{ON}/k_{OFF}, i.e., the proportion of time that the neurofilaments spend in the on track state, and the ratio k_A/k_R, i.e., the proportion of the time that the neurofilaments spend in the anterograde state

(see Figure 7). Thus we hypothesize that the decrease in transport velocity observed along lumbar spinal motor axons in mice and rats could be due to a decrease in the proportion of time that the filaments spend on track or an increase in the proportion of time that the filaments spend in the retrograde state. This could arise, for example, by spatial or temporal regulation of the binding or activity of the neurofilament motors. In future we plan to extend our modeling to address specifically the mechanisms that could account for temporal and spatial variations in transport velocity, because it is likely that such mechanisms are critical for regulating the steady state distribution of neurofilaments along axons. However, to test these hypotheses experimentally it will be necessary to develop new approaches that are capable of analyzing neurofilament pausing and directionality in vivo, which is a significant challenge.

The Relationship between Fast and Slow Axonal Transport

The average velocity of neurofilament transport excluding pauses is ~0.5 μm/s (Wang and Brown, 2001), which approaches the average velocity of membranous organelles in axons (Hill *et al.*, 2004). Thus it is possible that the cargoes of fast and slow axonal transport share similar or identical motors. In fact, there is now good evidence that dynein is the retrograde motor for neurofilaments (Shah *et al.*, 2000; Helfand *et al.*, 2003; Wagner *et al.*, 2004; He *et al.*, 2005) and dynein is also a known retrograde motor for membranous organelles (Vallee *et al.*, 2004). Likewise, conventional kinesin or its KIF5A isoform have been proposed to be the anterograde motor for neurofilaments (Yabe *et al.*, 1999; Helfand *et al.*, 2003; Xia *et al.*, 2003) and at least one of the KIF5 isoforms, KIF5B, is a known anterograde motor for some membranous organelles (Hirokawa and Takemura, 2005). In fact, the similarities between fast and slow axonal transport also extend to the pattern of movement itself. Direct observations on the movement of membranous organelles indicate that they can exhibit stop-and-go movements reminiscent of the behavior of neurofilaments (Zhou *et al.*, 2001; Zahn *et al.*, 2004) and the similarity is particularly striking for mitochondria, which move in a very intermittent manner (Hollenbeck, 1996; Ligon and Steward, 2000).

The fact that cargoes of fast and slow axonal transport are both conveyed by fast motors and can both exhibit stop-and-go movements might cause one to question whether there is really any difference between fast and slow axonal transport. In answer to this question, it is important to note that even though these distinct cargoes move at similar rates on a time scale of seconds or minutes, they clearly move at very different rates on a time scale of hours or days. However, this difference in overall rate is due primarily to differences in the amount of time spent pausing rather than to differences in the rate of movement. Thus the principal difference between fast and slow axonal transport is not the mechanism of movement per se but rather the mechanism by which the movement is regulated. Cytoskeletal and cytosolic protein complexes, including cytoskeletal polymers, form the slow components of axonal transport because they spend only a small fraction of their time moving. In contrast, membranous organelles such as Golgi-derived vesicles form the fast components of axonal transport because they spend a much higher proportion of their time moving. Thus the regulation of motor protein activity or motor-cargo interactions may be key to understanding the differences between fast and slow axonal transport (Brown, 2003).

ACKNOWLEDGMENTS

We thank Zuoshang Xu for providing the raw data from his published study on neurofilament transport in ventral root and sciatic nerve of mice. This work was funded by National Institutes of Health Grant NS-38526 to A.B. P.J. acknowledges the support of the Mathematical Biosciences Institute at Ohio State University (National Science Foundation Grant DMS-0098520), where he served as a Visiting Fellow during the time that some of this work was performed.

REFERENCES

Ackerley, S., Thornhill, P., Grierson, A. J., Brownlees, J., Anderton, B. H., Leigh, P. N., Shaw, C. E., and Miller, C. C. (2003). Neurofilament heavy chain side arm phosphorylation regulates axonal transport of neurofilaments. J. Cell Biol. *161*, 489–495.

Blum, J. J., and Reed, M. C. (1989). A model for slow axonal transport and its application to neurofilamentous neuropathies. Cell Motil. Cytoskelet. *12*, 53–65.

Brown, A. (2000). Slow axonal transport: stop and go traffic in the axon. Nat. Rev. Mol. Cell Biol. *1*, 153–156.

Brown, A. (2003). Axonal transport of membranous and nonmembranous cargoes: a unified perspective. J. Cell Biol. *160*, 817–821.

Francis, F., Roy, S., Brady, S. T., and Black, M. M. (2005). Transport of neurofilaments in growing axons requires microtubules but not actin filaments. J. Neurosci. Res. *79*, 442–450.

Glass, J. D., and Griffin, J. W. (1994). Retrograde transport of radiolabeled cytoskeletal proteins in transected nerves. J. Neurosci. *14*, 3915–3921.

He, Y., Francis, F., Myers, K. A., Yu, W., Black, M. M., and Baas, P. W. (2005). Role of cytoplasmic dynein in the axonal transport of microtubules and neurofilaments. J. Cell Biol. *168*, 697–703.

Helfand, B. T., Loomis, P., Yoon, M., and Goldman, R. D. (2003). Rapid transport of neural intermediate filament protein. J. Cell Sci. *116*, 2345–2359.

Hill, D. B., Plaza, M. J., Bonin, K., and Holzwarth, G. (2004). Fast vesicle transport in PC12 neurites: velocities and forces. Eur. Biophys. J. *33*, 623–632.

Hirokawa, N., and Takemura, R. (2005). Molecular motors and mechanisms of directional transport in neurons. Nat. Rev. Neurosci. *6*, 201–214.

Hoffman, P. N., Griffin, J. W., Gold, B. G., and Price, D. L. (1985). Slowing of neurofilament transport and the radial growth of developing nerve fibers. J. Neurosci. *5*, 2920–2929.

Hoffman, P. N., Lasek, R. J., Griffin, J. W., and Price, D. L. (1983). Slowing of the axonal transport of neurofilament proteins during development. J. Neurosci. *3*, 1694–1700.

Hollenbeck, P. J. (1996). The pattern and mechanism of mitochondrial transport in axons. Front. Biosci. *1*, d91–d102.

Jung, C., and Shea, T. B. (1999). Regulation of neurofilament axonal transport by phosphorylation in optic axons in situ. Cell Motil. Cytoskelet. *42*, 230–240.

Jung, P., Kissner, J. G., and Hanggi, P. (1996). Regular and chaotic transport in asymmetric periodic potentials: inertia ratchets. Phys. Rev. Lett. *76*, 3436–3439.

LaMonte, B. H., Wallace, K. E., Holloway, B. A., Shelly, S. S., Ascano, J., Tokito, M., Van Winkle, T., Howland, D. S., and Holzbaur, E. L. (2002). Disruption of dynein/dynactin inhibits axonal transport in motor neurons causing late-onset progressive degeneration. Neuron *34*, 715–727.

Lasek, R. J., Garner, J. A., and Brady, S. T. (1984). Axonal transport of the cytoplasmic matrix. J. Cell Biol. *99*, 212s–221s.

Lasek, R. J., Paggi, P., and Katz, M. J. (1992). Slow axonal transport mechanisms move neurofilaments relentlessly in mouse optic axons. J. Cell Biol. *117*, 607–616.

Ligon, L. A., and Steward, O. (2000). Movement of mitochondria in the axons and dendrites of cultured hippocampal neurons. J. Comp. Neurol. *427*, 340–350.

Nixon, R. A. (1998). The slow axonal transport of cytoskeletal proteins. Curr. Opin. Cell Biol. *10*, 87–92.

Nixon, R. A., and Logvinenko, K. B. (1986). Multiple fates of newly synthesized neurofilament proteins: evidence for a stationary neurofilament network distributed non-uniformly along axons of retinal ganglion cells. J. Cell Biol. *102*, 647–659.

Ochs, S. (1975). A unitary concept of axoplasmic transport based on the transport filament hypothesis. In: Recent Advances in Myology: Proceedings of the Third International Congress on Muscle Diseases, ed. W. G. Bradley, D. Gardner-Medwin, and J. N. Walton, Amsterdam: Excerpta Medica, 189–194.

Press, W. H., Flannery, B. P., Teukolsky, S. A., and Vetterling, W. T. (1992). Numerical Recipes in Fortran, New York: Cambridge University Press.

Price, R. L., Paggi, P., Lasek, R. J., and Katz, M. J. (1988). Neurofilaments are spaced randomly in the radial dimension of axons. J. Neurocytol. *17*, 55–62.

Reles, A., and Friede, R. L. (1991). Axonal cytoskeleton at the nodes of Ranvier. J. Neurocytol. *20*, 450–458.

Roy, S., Coffee, P., Smith, G., Liem, R.K.H., Brady, S. T., and Black, M. M. (2000). Neurofilaments are transported rapidly but intermittently in axons: implications for slow axonal transport. J. Neurosci. *20*, 6849–6861.

Shah, J. V., Flanagan, L. A., Janmey, P. A., and Leterrier, J.-F. (2000). Bidirectional translocation of neurofilaments along microtubules mediated in part by dynein/dynactin. Mol. Biol. Cell *11*, 3495–3508.

Tytell, M., Black, M. M., Garner, J. A., and Lasek, R. J. (1981). Axonal transport: each major component reflects the movement of distinct macromolecular complexes. Science *214*, 179–181.

Vallee, R. B., Williams, J. C., Varma, D., and Barnhart, L. E. (2004). Dynein: an ancient motor protein involved in multiple modes of transport. J. Neurobiol. *58*, 189–200.

Van Kampen, N. G. (1981). Stochastic Processes in Physics and Chemistry, New York: North Holland.

Wagner, O. I., Ascano, J., Tokito, M., Leterrier, J. F., Janmey, P. A., and Holzbaur, E. L. (2004). The interaction of neurofilaments with the microtubule motor cytoplasmic dynein. Mol. Biol. Cell *15*, 5092–5100.

Wang, L., and Brown, A. (2001). Rapid intermittent movement of axonal neurofilaments observed by fluorescence photobleaching. Mol. Biol. Cell *12*, 3257–3267.

Wang, L., Ho, C.-L., Sun, D., Liem, R.K.H., and Brown, A. (2000). Rapid movement of axonal neurofilaments interrupted by prolonged pauses. Nat. Cell Biol. *2*, 137–141.

Watson, D. F., Glass, J. D., and Griffin, J. W. (1993). Redistribution of cytoskeletal proteins in mammalian axons disconnected from their cell bodies. J. Neurosci. *13*, 4354–4360.

Wujek, J. R., Lasek, R. J., and Gambetti, P. (1986). The amount of slow axonal transport is proportional to the radial dimensions of the axon. J. Neurocytol. *15*, 75–83.

Xia, C. H., Roberts, E. A., Her, L. S., Liu, X., Williams, D. S., Cleveland, D. W., and Goldstein, L. S. (2003). Abnormal neurofilament transport caused by targeted disruption of neuronal kinesin heavy chain KIF5A. J. Cell Biol. *161*, 55–66.

Xu, Z., and Tung, V. W. (2000). Overexpression of neurofilament subunit M accelerates axonal transport of neurofilaments. Brain Res. *866*, 326–332.

Xu, Z., and Tung, V. W. (2001). Temporal and spatial variations in slow axonal transport velocity along peripheral motoneuron axons. Neuroscience *102*, 193–200.

Yabe, J. T., Pimenta, A., and Shea, T. B. (1999). Kinesin-mediated transport of neurofilament protein oligomers in growing axons. J. Cell Sci. *112*, 3799–3814.

Yabe, J. T., Chan, W.K.-H., Chylinski, T. M., Lee, S., Pimenta, A., and Shea, T. B. (2001). The predominant form in which neurofilament subunits undergo axonal transport varies during axonal initiation, elongation and maturation. Cell Motil. Cytoskelet. *48*, 61–83.

Zahn, T. R., Angleson, J. K., MacMorris, M. A., Domke, E., Hutton, J. F., Schwartz, C., and Hutton, J. C. (2004). Dense core vesicle dynamics in *Caenorhabditis elegans* neurons and the role of kinesin UNC-104. Traffic *5*, 544–559.

Zhou, H. M., Brust-Mascher, I., and Scholey, J. M. (2001). Direct visualization of the movement of the monomeric axonal transport motor UNC-104 along neuronal processes in living *Caenorhabditis elegans*. J. Neurosci. *21*, 3749–3755.